Sub-critical filtration conditions of commercial hollow-fibre membranes in a submerged anaerobic MBR (HF-SAnMBR) system: the effect of gas sparging intensity

A. Robles[a,*], M.V. Ruano[b], F. García-Usach[a] and J. Ferrer[a]

[a] Institut Universitari d'Investigació d'Enginyeria de l'Aigua i Medi Ambient, IIAMA, Universitat Politècnica de València, Camí de Vera s/n, 46022, Valencia, Spain (e-mail: *ngerobma@upv.es; magarus@hma.upv.es; jferrer@hma.upv.es*)

[b] Departament d'Enginyeria Química, Escola Tècnica Superior d'Enginyeria, Universitat de València, Avinguda de la Universitat s/n, 46100, Burjassot, Valencia, Spain (e-mail: *m.victoria.ruano@uv.es)*

* Corresponding author: tel. +34 96 387 99 61, fax +34 96 387 90 09, e-mail: *ngerobma@upv.es*

Abstract

A submerged anaerobic MBR demonstration plant with two commercial hollow-fibre ultrafiltration systems (PURON®, Koch Membrane Systems, PUR-PSH31) was operated using municipal wastewater at high levels of mixed liquor total solids (MLTS) (above 22 g L^{-1}). A modified flux-step method was applied to assess the critical flux (J_C) at different gas sparging intensities. The results showed a linear dependency between J_C and the specific gas demand per unit of membrane area (SGD_m). J_C ranged from 12 to 19 LMH at SGD_m values of between 0.17 and 0.5 $Nm^3\ h^{-1}\ m^{-2}$, which are quite low in comparison to aerobic MBR. Long-term trials showed that the membranes operated steadily at fluxes close to the estimated J_C, which validates the J_C obtained by this method. After operating the membrane for almost two years at sub-critical levels, no irreversible fouling problems were detected, and therefore, no chemical cleaning was conducted.

Keywords

Critical flux; gas sparging; industrial hollow-fibre membranes; modified flux-step

method; submerged anaerobic membrane bioreactor

1. Introduction

In recent years there has been increased interest in assessing the feasibility of the anaerobic treatment of municipal wastewater at ambient temperature conditions. This interest focusses on the sustainability advantages of anaerobic rather than aerobic processes, i.e. low sludge production due to the low anaerobic biomass yield; low energy consumption because no aeration is needed; and the generation of biogas which can be used as an energy resource. The total greenhouse emissions of this technology are, therefore, low because low energy consumption indirectly means low gas emissions. The main challenge of anaerobic biotechnology is to develop treatment systems that prevent biomass loss and enable high sludge retention times (SRT) in order to offset the low growth rates of anaerobic biomass at ambient temperatures (Lin *et al*., 2010). In this respect, anaerobic membrane bioreactors (AnMBR) are a promising technology for municipal wastewater treatment. Furthermore, the membrane separation process allows high organic loading to be obtained with municipal wastewater, since low COD levels are remedied by high treatment flow rates in small reaction volumes: something not possible with classical anaerobic systems (UASB and EGSB). However, operating membrane bioreactors with high SRTs may mean operating at high mixed liquor total solid (MLTS) levels: one of the main constraints of using membranes (Judd, 2010). These high MLTS levels contribute to membrane fouling: the key issue of membrane technology. Fouling decreases membrane permeability (K) and increases operating and maintenance costs (Chang *et al*., 2002). It is important to emphasise that AnMBR systems enable membranes to operate at MLTS levels higher than in aerobic MBRs because anaerobic MBRs do not have the oxygen transfer constraints that limit

MLTS levels in aerobic MBRs (Stephenson *et al.*, 2000). In this respect, a considerable reduction in the design operating volume can be achieved in comparison with the volume required in aerobic conditions.

The key operating challenge in AnMBR technology is to optimise membrane operating in order to minimise any kind of membrane fouling and thereby increase the membrane lifespan. The gas sparging intensity in each operating range is a key operating parameter that must be optimized in order to minimise both investment and operating costs in AnMBR systems. Several strategies to control fouling (Liao *et al.*, 2006; Vallero *et al.*, 2005; Dvořák *et al.*, 2011) aim to optimise filtration whilst minimising investment and operating costs. One such strategy is based on using membranes in sub-critical filtration conditions. These conditions are limited by the critical flux (J_C): a quantitative filtration parameter defined firstly as "the flux below which no fouling occurs" (Bachin *et al.*, 1995), or as "the flux below which a decline of flux with time does not occur; above it, fouling is observed" (Field *et al.*, 1995). On the basis of these definitions, two different concepts have developed. In the "strong" concept, critical flux (J_{CS}) is defined as the flux below which membrane performance is equal to its ability to treat clean water under same operating conditions. In the "weak" concept, critical flux (J_{CW}) is defined as the flux (not necessarily the same as the clean-water flux) below which the transmembrane pressure (TMP) and J are not directly related.

Different methodologies to determine J_C have been reported in literature, the flux-step method being the most common (Le-Clech *et al.*, 2003; Guglielmi *et al.*, 2007; van der Marel *et al.*, 2009). This method enables J_C to be determined in a wide range of operating conditions, mainly in relation to the level of MLTS or gas sparging intensity,

usually measured as specific gas demand per unit of membrane area (SGD_m). MLTS level and gas sparging intensity have both been identified as the factors that affect J_C most. Furthermore, it has been pointed out that the J_C resulting from the flux-step method cannot be used to estimate the critical flux of full-scale systems operated continuously because it is a short-term estimate usually made off line (Le-Clech *et al*., 2003).

Several published studies provide the J_C of both aerobic and anaerobic MBRs on a laboratory scale (Guglielmi *et al*., 2006; Jeison *et al*., 2006; Delgado *et al*., 2008). However, further studies are needed in order to determine the J_C of submerged AnMBR (SAnMBR) technology on a semi-industrial scale. Moreover, the effect of the main operating conditions on membrane fouling cannot be evaluated properly at the lab scale because they depend heavily on the membrane size. In hollow-fibre (HF) membranes in particular the HF length is a critical parameter. Therefore, since membrane performance cannot be scaled up directly from laboratory to plant dimensions, especially in the case of HF-based technology, further studies of HF-SAnMBR technology on an industrial scale are needed in order to facilitate its design and implementation in full-scale wastewater treatment plants (WWTP).

To gain more insight into the optimisation of the physical separation process in a SAnMBR system on an industrial scale, our study evaluated the critical filtration conditions of industrial HF membranes. In order to obtain robust results that can be extrapolated to full-scale plants, a SAnMBR system featuring industrial HF membrane units was operated using effluent from the pre-treatment of the Carraixet WWTP (Valencia, Spain). The main objective of this study was to assess the ability of the flux-step method to predict the critical flux in continuous full-scale HF-SAnMBR operations

and validate the J_C values obtained during the long-term operating of membranes in sub-critical conditions. Furthermore, the effect of the gas sparging intensity on both membrane performance and J_C was studied whilst operating the membranes with high levels of MLTS.

2. Materials and methods

2.1. Demonstration plant description

Figure 1a shows the HF-SAnMBR demonstration plant used in this study. It consists of an anaerobic reactor with a total volume of 1.3 m^3 (0.4 m^3 head space) connected to two membrane tanks each with a total volume of 0.8 m^3 (0.2 m^3 head space). Each membrane tank has one industrial HF ultrafiltration membrane unit (PURON®, Koch Membrane Systems (PUR-PSH31) with 0.05 µm pores). Each module has 9 HF bundles, 1.8 m long, giving a total membrane surface of 30 m^2. Normal membrane operating consists of a specific schedule involving a combination of different individual stages taken from a basic filtration-relaxation (F-R) cycle. Besides classical membrane operating stages (filtration, relaxation and back-flush), two additional stages were also considered in membrane operating: degasification and ventilation (Giménez *et al.*, 2011).

Figure 1b shows the flow diagram of the HF-SAnMBR demonstration plant. It is fed with the effluent from the Carraixet WWTP pre-treatment (screening, degritter, and grease removal). After further pre-treatment in the rotofilter (RF) and homogenisation in the equalisation tank (ET), the wastewater is pumped to the anaerobic reactor (AnR). In order to improve the stirring conditions of the anaerobic reactor and to favour the

stripping of the produced gases from the liquid phase, a fraction of the produced biogas is recycled to this reactor. The sludge is continuously recycled through the external membrane tanks (MT) where the effluent is obtained by vacuum filtration. In order to minimise the cake layer formation, another fraction of the produced biogas is also recycled to the membrane tanks from the bottom of each fibre bundle.

For further details about this SAnMBR demonstration plant see Giménez *et al*. (2011).

2.2. Demonstration plant monitoring

Numerous on-line sensors and items of automatic equipment were installed in order to automate and control demonstration plant operations and provide on-line information about the state of the process. Specifically, the on-line sensors assigned to each membrane tank consist of: 1 pH-temperature transmitter (Endress+Hauser Orbisint CPS11D Memosens); 1 level indicator transmitter (Endress+Hauser Waterpilot FMX167); 1 flow indicator transmitter for the mixed liquor feed pump (Endress+Hauser Promag 50W); 1 flow indicator transmitter for the permeate pump (Endress+Hauser Promag 50P); and 1 liquid pressure indicator transmitter to control the TMP (Endress+Hauser Cerabar M PMC41). The group of actuators assigned to each membrane tank consists of a group of on/off control valves which determine the direction of the flow in order to control the different membrane operating stages (filtration, back-flush, relaxation…), and 3 frequency converters (Micromaster Siemens 420). Each frequency converter controls the rotational speed of the permeate pump (JUROP VL02 NBR), the mixed liquor feed pump (CompAir NEMO), and the membrane tank blower (FPZ 30HD).

Besides the on-line process monitoring, in order to assess the performance of the biological process, 24-hour composite samples were taken from influent and effluent streams, and grab samples of anaerobic sludge were taken once a day. The following parameters were analysed daily in influent stream: total suspended solids (TSS); volatile suspended solids (VSS); volatile fatty acids (VFA) concentration; carbonate alkalinity (Alk); and nutrients (ammonium (NH_4-N) and orthophosphate (PO_4-P)); the following parameters were analysed daily in effluent stream: VFA concentration; carbonate alkalinity; and nutrients (NH_4-N and PO_4-P); and the following parameters were analysed daily in mixed liquor: total solids (MLTS); volatile solids (MLVS); VFA concentration; carbonate alkalinity; and nutrients (NH_4-N and PO_4-P). The total and soluble chemical oxygen demand (COD_T and COD_S, respectively) were determined once a week in both influent and effluent streams, and mixed liquor. In addition, the total and soluble biological oxygen demand (BOD_T and BOD_S, respectively) were determined once a week in both influent and effluent streams in order to get an idea of the aerobically biodegradable fraction of organic matter that is anaerobically removed in the system.

2.3. Demonstration plant operation

The start-up of the demonstration plant was carried out with biomass inoculum (40% of the working volume) coming from a full-scale anaerobic digester.

The long-term operation of this SAnMBR system was conducted at different SRTs (from 30 to 70 days), hydraulic retention times (HRTs) ranged from 6 to 26 hours, and organic loading rates (OLR) between 0.3 and 1.1 kgCOD m^{-3} d^{-1}. The temperature

varied from 33 to 17 ºC. The pH of the mixed sludge throughout this period ranged from 6.5 to 7.1. The MLTS level ranged from around 10 to 30 g L^{-1}. With regard to the physical separation process, J_{20} was varied from 9 to 13.3 LMH, with SGD_m values from around 0.23 to 0.33 Nm^3 h^{-1} m^{-2}. The cross-flow sludge velocity over the membrane surface was set to 3.6 mm s^{-1}, giving a sludge flow rate through the membrane module of 2700 L h^{-1}. The membrane operating mode was: a 300-second basic F-R cycle (250 s filtration and 50 s relaxation), 30 seconds of back-flush every 10 F-R cycles, 40 seconds of ventilation every 10 F-R cycles, and 30 seconds of degasification every 50 F-R cycles.

The specific operating conditions corresponding to the short-term trials were: an SRT of 70 days; controlled temperature of 33 ºC; and a MLTS level in the sludge fed to the membrane tank of 23 g L^{-1}.

Important to highlight is the wide variation in the anaerobic reactor influent loads during the experiment (i.e. 186 ± 61 mg L^{-1} of TSS or 388 ± 95 mg L^{-1} of Total COD), reflected by the high standard deviation of each parameter.

2.4. Analytical methods

2.4.1. Analytical monitoring

Total solids, volatile solids, total suspended solids, volatile suspended solids, COD_T and COD_S, BOD_T and BOD_S, NH_4-N, and PO_4-P were determined according to Standard Methods (2005) and using the following approaches for each parameter: 2540 B, 2540 E, 2540 D, 2540 E, 5220 B and 5220 D, 5210 B and 5210 C, 4500-NH3 G, and

4500-P E, respectively. Carbonate alkalinity and VFA concentration were determined by titration according to the method proposed by WRC (1992). The methane fraction of the biogas was measured using a gas chromatograph equipped with a Flame Ionization Detector (GC-FID, Thermo Scientific). 1 mL of biogas was collected by a gas-tight syringe and injected into a 30 m x 0.319 mm x 25 µm HP-MOLESIEVE column (Agilent Technologies) that was maintained at 40 ºC. The carrier gas was helium at a flow-rate of 40 mL min^{-1}. CH4 pure gas (99.9995%) was used as standard. Particle size distribution was obtained using a Mastersizer2000 coupled to a Hydro 2000SM (A) with a detection range of 0.02 to 2000 µm.

2.4.2. Modified flux-step method and membrane performance indices

The 20 ºC-normalised membrane permeability (K_{20}) was calculated using a simple filtration model (Eq. 1) that takes into account the on-line monitored data of TMP and J. This simple filtration model includes temperature correction (Eq. 2) to account for the dependence of permeate viscosity on temperature (Rosenberger *et al.*, 2006), and therefore the normalised flux (J_{20}) was obtained by using Eq. 4. Total membrane resistance (R_T) was theoretically represented by the following partial resistances (Eq. 3): membrane resistance (R_M); cake layer resistance (R_C); and irreversible layer resistance (R_I).

$$K_{20} = \frac{1}{\eta \cdot R_T} = \frac{J_T f_T}{TMP} \quad \text{(Eq. 1)}$$

$$f_T = e^{-0.0239\,(T-20)} \quad \text{(Eq. 2)}$$

$$R_T = R_m + R_c + R_I \quad \text{(Eq. 3)}$$

$$J_{20} = J_T \cdot e^{-0.0239\,(T-20)} \quad \text{(Eq. 4)}$$

In our study, J_{CW} (critical flux in the weak definition, as stated before) was determined by applying a modified flux-step method based on the method proposed by van der Marel *et al*. (2009). This modified method (see Figures 2a and 2b) establishes successive flux-steps analogous to the common flux-step method. The duration of the filtration stage was set to 15 minutes. The flux-step size was arbitrarily set to a J_{20} of 1.22 LMH, and downward flux-stepping was started when a maximum TMP threshold value was reached (0.4 bars). In order to reduce the effect of reversible fouling on J_{CW} calculations, a relaxation stage of 15 minutes was inserted between each flux-step. The relaxation stages were conducted using the same SGD_m as in the filtration stages. In this study, five flux-step tests were carried out at an SGD_m of 0.17, 0.23, 0.33, 0.4 and 0.5 $Nm^3\ h^{-1}\ m^{-2}$.

In a way similar to the approach suggested by several authors (Stephenson *et al.*, 2000; Le-Clech *et al.*, 2003), the data processing of the results from the flux-step method used the derived parameters shown in equations 5 to 8. Eq. 5 and Eq. 6 give the average values of TMP and K_{20} for each flux-step (J^n), respectively. Eq. 7 is the difference in TMP at the same J_{20} between upward flux-stepping and downward flux-stepping (see Figure 2c). The fouling rate (Eq. 8) was calculated as the increase in TMP in individual filtration stages.

$$TMP_{J^n}^{AVE} = \left(\sum_{j=1}^{z} TMP_{J^n}^{j}\right)/\sum z \qquad \text{(Eq. 5)}$$

$$K_{20_{J^n}}^{AVE} = \left(\sum_{j=1}^{z} K_{20_{J^n}}^{j}\right)/\sum z \qquad \text{(Eq. 6)}$$

$$\Delta TMP_{AVE} = \left(TMP_{J^n}^{AVE}\right)^{DOWNWARD} - \left(TMP_{J^n}^{AVE}\right)^{UPWARD} \qquad \text{(Eq. 7)}$$

$$\frac{dTMP}{dt} \approx \frac{\Delta \mathrm{TMP}}{\Delta t} = \frac{TMP_{J^n}^{f} - TMP_{J^n}^{i}}{t_{J^n}^{f} - t_{J^n}^{i}} \qquad \text{(Eq. 8)}$$

3. Results and discussion

This study entailed short-term and long-term trials. In the short-term trials, SGD_m ranged from 0.17 to 0.50 $Nm^3 h^{-1} m^{-2}$, whilst J_{20} varied from around 9.5 to 20.5 LMH. In these short-term trials the MLTS level in the anaerobic sludge entering the membrane tank was 23 g L^{-1}. It must be emphasised that the MLTS level in the membrane tank increased according to the ratio between the membrane tank sludge intake and the net permeate flow rate (the MLTS level in the membrane tank was around 26 g L^{-1}).

3.1. Short-term trials: Effect of SGD_m on membrane performance

Figure 3 shows the results of the short-term trials of both TMP_{AVE} and $K_{AVE,20}$ obtained by applying Eq. 5 and Eq. 6, respectively. As Figure 3a shows, the effect of J_{20} on TMP_{AVE} becomes evident at levels of above 13 LMH, there being no obvious relationship below this level. This behaviour highlights the need to optimise the physical separation process at every operating range, since considerable energy savings could be achieved. For instance, Figure 3a shows that it is theoretically possible to operate the membranes at SGD_m of 0.17 $Nm^3 h^{-1} m^{-2}$ when operating at a J_{20} of less than 13 LMH: a value far lower than the lower threshold in the typical operating range for aerobic processes suggested by the membrane supplier (0.3 $Nm^3 h^{-1} m^{-2}$). This figure shows that the higher the J_{20}, the greater the effect of SGD_m on TMP_{AVE}. When J_{20} is higher than 13 LMH, an increase in SGD_m from 0.17 to 0.33 $Nm^3 h^{-1} m^{-2}$ affects TMP_{AVE} considerably but a further increase to 0.5 $Nm^3 h^{-1} m^{-2}$ has no significant effect at J_{20} values lower than 15.8 LMH. Thus, an SGD_m of 0.5 $Nm^3 h^{-1} m^{-2}$ would only be needed at J_{20} values of more than 18 LMH. It must be said that the maximum SGD_m studied (0.5 $Nm^3 h^{-1} m^{-2}$) is lower than the upper threshold in the typical operating range

for aerobic processes suggested by the membrane supplier (0.7 $Nm^3\ h^{-1}\ m^{-2}$).

Figure 3b shows how at similar J_{20} values the resulting $K_{AVE,20}$ decreases as SGD_m decreases. A flux of J_{20} = 15.8 LMH, for instance, resulted in a $K_{AVE,20}$ of 70, 90, and 110 LMH bar^{-1} at an SGD_m of 0.17, 0.33 and 0.5 $Nm^3\ h^{-1}\ m^{-2}$, respectively. It must be said that the K_{20} values predicted by these short-term trials are quite high taking into account the relatively high J_{20} applied and the low SGD_m applied. For instance, the K_{20} values of full-scale aerobic MBR plants treating domestic wastewater are generally between 150 and 250 LMH bar^{-1}, whilst the applied SGD_m is usually higher when operating at similar J_{20} values (Judd, 2010). On the other hand, it is well known that K_{20} depends considerably on the applied SGD_m. This dependency is related mainly to the contribution of the reversible fouling component (related to R_C) to the R_T. In this respect, the higher K_{20} obtained in the series of experiments conducted with an SGD_m level of 0.5 $Nm^3\ h^{-1}\ m^{-2}$ was related to the lowest cake layer formation rate. It must be said that according to the conceptual filtration model, two different effects determine R_C: the cake layer formation rate (due to the filtration process) and the cake layer removal rate (due mainly to biogas sparging). Thus, at an established MLTS concentration the cake layer removal efficiency decreases as SGD_m decreases. In this respect, long-term operating with a considerable amount of cake layer on the membrane surface throughout successive filtration stages could result in a higher propensity to irreversible fouling (related to R_I), due to greater cake layer formation and consolidation on the membrane surface.

3.2. Short-term trials: Effect of SGD_m on J_{CW}

Figure 4a shows the fouling rates (calculated using Eq. 8) during the short-term

trials carried out at a MLTS of 23 g L^{-1} and different SGD_m levels. This figure shows the effect of the gas sparging intensity upon the membrane fouling rate at different values of J_{20}. It can be seen that there is a minimum J_{20} value (around 13 LMH) below which the fouling rate seems to be independent of both J_{20} and SGD_m. However, when J_{20} was above 13 LMH then the effect of J_{20} on the fouling rate declined when SGD_m increased. For instance, at a J_{20} of 12 LMH it is theoretically possible to operate membranes sub-critically with a gas sparging intensity of 0.17 $Nm^3\ h^{-1}\ m^{-2}$, a value that has to be increased to 0.5 $Nm^3\ h^{-1}\ m^{-2}$ in order to achieve a J_{20} of 19 LMH. These results predict that it is theoretically possible to maintain sub-critical filtration conditions (i.e. to operate at sustainable J_{20} values) when operating membranes at quite high MLTS levels, without applying a prohibitive SGD_m.

As mentioned before, these results confirm that the optimisation of the physical separation process in every operating range will result in significant energy savings in HF-SAnMBR systems. On the other hand, Figure 4b shows J_{CW} to be directly related to SGD_m at the selected operating conditions. This relationship predicts that it is theoretically possible to operate membranes sub-critically when J_{20} is between 12 and 19 LMH, and when SGD_m ranges from 0.17 to 0.50 $Nm^3\ h^{-1}\ m^{-2}$. Thus, a considerable increase in J_{20} can be achieved in sub-critical filtrations conditions by increasing SGD_m just slightly.

Table 1 summarises some of the J_C values found in literature under different operating conditions: membrane type and pore size, wastewater feed, MBR system, operating MLTS level, and air/gas sparging intensity. In contrast with other publications, results from our study revealed J_C to be closely related to SGD_m, as shown by the linear regression in Figure 4b. The high pseudoplastic behaviour of the sludge at

high MLTS levels must be mentioned. In this respect, a considerable decrease in sludge viscosity was recorded by a rotation viscometer (from about 8000 to 400 cp) when the velocity gradient was increased (from 0.1 to 5 s^{-1}, respectively). This non-Newtonian behaviour of sludge may explain the significant increase in J_C when SGD_m increased. Guglielmi *et al*. (2007) observed a slight dependency under aerobic conditions for MLTS concentrations of 10 g L^{-1}. The J_C values obtained by these authors were higher than those obtained in this study due to the lower operating MLTS level and the higher SGD_m applied. These results tally well with the behaviour observed in this study, which showed that above a certain SGD_m value the fouling rate becomes independent of J_{20} at a specific MLTS level. Howell *et al*. (2004) obtained critical flux values ranging from 10 to 20 LMH (aerobic MBR, MLTS of 20 g L^{-1}, and upward airflow velocity (U_G) between 25 and 200 mm s^{-1}). These results are in agreement with the J_C values obtained in our study (carried out under similar conditions). Nevertheless, it is important to highlight that the results in Table 1 were obtained in laboratories and cannot, therefore, be automatically applied directly to full-scale plants since the effect of gas sparging upon membrane fouling depends considerably on fibre length and hydrodynamic conditions in membrane tanks.

These results confirm the need to optimise the gas sparging intensity for both every operating range and every membrane operating mode. As mentioned before, this enables not only considerable energy savings but also adequate long-term operating since it is possible to minimise the onset of irreversible fouling problems. In this respect, the main operating factors affecting membrane fouling should be also assessed: frequency and duration of the physical cleaning stages (back-flush and relaxation); treatment flow rate (which affects the J and thus the sub-critical filtration conditions); MLTS levels, which also affect the sub-critical conditions considerably; and cross-flow

sludge velocity, which affects not only the removal of the cake layer but also the MLTS level in the membrane tank. Hence, it is essential to control the gas sparging to ensure adequate membrane scouring and thereby optimise the economic feasibility of HF membranes in SAnMBR systems.

3.3. Short-term trials: Effect of SGD_m on residual TMP

It has been observed by other authors that an increase in the average TMP (ΔTMP_{AVE}) at identical J_{20} can be obtained, between upward flux-stepping and downward flux-stepping (see Figure 2c). This increase could be related to "how much gas scouring is able to mechanically limit the extent of irreversible fouling due to the overcoming of the critical flux" (Delgado *et al.*, 2008). Despite non-clear dependencies having been observed in our study between both ΔTMP_{AVE} and J_{20} in each flux-step, a direct dependency between the final ΔTMP_{AVE} and the J_{CW20} obtained in each short-term trial was observed (see Figure 4c). As shown in this figure, the higher the J_{CW20} obtained, the higher the residual TMP at the end of the short-term trial. This dependency reveals that SGD_m values higher than those resulting from the flux-step method are needed in order to minimise the possibility of membranes being irreversibly fouled during long-term operating. In this respect, membranes operating continuously at J_{20} levels similar to the theoretical J_{CW20} values calculated for the flux-step method could result in the incomplete removal of the cake layer from the membrane surface. This incomplete removal increases the propensity of the cake layer to consolidate on the membrane surface, thus irreversible fouling may tend to increase. Hence, a higher SGD_m might be necessary when membranes are operated under near-critical conditions. For this reason, a critical flux security factor (ζ_{CF}) for long-term operation is recommended in our study. The ζ_{CF} values range from 0 to 1 (0.75 to 0.95 is the range

recommended in our study). This factor multiplies the J_{CW20} value obtained in experiments, setting an operating J_{20} lower than the critical value predicted by the flux-step method. Hence, the main aim of this ζ_{CF} is to operate membranes sub-critically in order to minimise the possibility of irreversible fouling problems.

3.4. Long-term trials: Assessment of sub-critical filtration conditions

As mentioned before, it has been pointed out by several authors that the J_C resulting from the flux-step method cannot be used to estimate the critical flux in continuously operated full-scale systems because it is usually determined during a short-term experiment normally carried out off-line. However, this limitation was reduced in our study because the flux-step method was carried out with industrial membranes operating with real municipal wastewater and, therefore, with a biomass population and mixed liquor properties similar to those expected during long-term membrane operating. In addition, the following limiting factors related to the membrane size have been overcome: (1) membrane length, which is well-known to affect not only shear conditions and gas sparging efficiency, but also the TMP needed due to the axial pressure differential; (2) packaging density, which affects the hydrodynamics of the membrane tank considerably, and specifically the space inside the membrane package structure; and (3) the grade of lateral movement, which is affected considerably by the membrane module length and contributes to removing the cake layer. Thus, differences between the theoretical J_C values (calculated using the flux-step method) and those observed in long-term experiments have been reduced in this study. Hence, the membranes were seen to operate steadily at fluxes close to the theoretical J_C value.

Different long-term trials were carried out in order to assess the performance of

membranes at specific sub-critical conditions similar to those expected in full-scale plants (i.e. variations in MLTS levels, variations in influent loads, etc). Figure 5 shows the K_{20} obtained in the long-term trials carried out with a J_{20} value of 10 LMH (Figure 5a) and 13.3 LMH (Figure 5b). The SGD_m in these long-term trials was 0.23 and 0.33 $Nm^3\ h^{-1}\ m^{-2}$ respectively. The J_{CW20} of these SGD_m and MLTS of 23 g L^{-1} resulted in 13 and 15 LMH, respectively. This figure also includes the MLTS level of the sludge fed to the membrane tank throughout the experimental periods. As mentioned before, this MLTS level increased in the membrane tank (up to 5 g L^{-1}) according to the ratio between the sludge flow-rate entering the membrane tank and the net permeate flow rate. It is important to note the considerable variation in MLTS levels (from around 22 to 30 g L^{-1}) in the SAnMBR system throughout the long-term trials, due to considerable fluctuations in the influent load (i.e. 186 ± 61 mg L^{-1} of TSS). This figure shows the considerable effect of MLTS levels on K_{20} during the two experimental periods using different J_{20}. Every variation in the MLTS level was inversely reflected in the K_{20}. Nevertheless, even with high MLTS levels (up to 25 g L^{-1}), K_{20} remained at sustainable values (above 100 LMH bar^{-1}). This figure also shows that stable MLTS concentrations give quite stable K_{20} values. The stability of K_{20} could be attributed to the low TMP achieved during this period (around 0.1 bars), which illustrates low membrane and cake layer compression, resulting in a stable R_M value and an R_C value that only depends on the thickness of the cake layer, respectively. Moreover, the K_{20} improved when the MLTS decreased (see Figure 5b), which indicates the absence of an irreversible fouling component (related to R_I) on R_T. Therefore, only the dynamic component R_C was detected in this experimental period.

The results of this study suggest that sub-critical filtration conditions together with an adequate schedule of the different physical cleaning stages of membranes (relaxation

and back-flush) enable long-term membrane operating and minimise the possibility of irreversible fouling problems. On the other hand, operating membranes with a suitable ζ_{CF} value could minimise the appearance of filtration problems. In this study, a ζ_{CF} ranging from around 80 to 90% was established for both 10 and 13.3 LMH long-term trials. It is a well-known fact that working with a ζ_{CF} could cause the design of MBR plants to be overdimensioned since a higher total filtration area is required for a specific J_{20}. However, this larger filtration area causes an increase in the membrane lifespan. Hence, a reduction in replacement and maintenance costs can be achieved. In this respect, after almost two years of operating the membranes at sub-critical levels, no irreversible fouling problems were detected, even at high MLTS levels.

Figure 6 shows the TMP profile obtained during the long-term operating period, as well as the MLTS level in the anaerobic sludge fed to the membrane tank. Both TMP and MLTS level are referred to its daily average value. This figure illustrates how the TMP was maintained at low values (around 0.1 bars) even for high MLTS levels (up to 25 g L^{-1}). Above this value, the TMP showed a sharp increase when the critical filtration conditions were exceeded. In fact, the TMP reached considerable high values (above 0.3 bars) for MLTS levels around 30 g L^{-1}. It is important to emphasise that it was possible to operate membranes at low TMP with relatively low SGD_m values (around 0.23 Nm^3 h^{-1} m^{-2}), even at high MLTS levels (up to 25 g L^{-1}).

The membranes therefore required non-chemical cleaning, mainly due to both operating in sub-critical filtration conditions and establishing an adequate membrane operating mode. However, further research is needed in order to gather more information about different operating conditions, information which will be necessary in order to carry out an exhaustive economic analysis of the proposed technology in

comparison with existing technologies.

Finally, with regard to the biological process performance, in general low effluent VFA concentrations (< 30 mg COD L^{-1}), as well as significant methane-rich (over 70% v/v) biogas productions were observed (around 100 L d^{-1} in average), which evidenced a suitable biological process performance. Overall, high treatment efficiencies in term of COD removal were achieved (around 85 %). Further details on the biological process performance of this SAnMBR system can be found in Giménez et al. (2011).

4. Conclusions

The results of this study suggest that HF-SAnMBR technology is promising for municipal wastewater treatment since it can consume less energy than aerobic MBRs. A linear dependency between the J_C and the SGD_m was observed. At MLTS above 22 g L^{-1}, J_C ranged from 12 to 19 LMH at quite low SGD_m values compared to aerobic MBRs (between 0.17 and 0.5 $Nm^3\ h^{-1}\ m^{-2}$, respectively). Long-term trials suggested that operating in sub-critical filtration conditions and an adequate operating mode can result in adequate and sustainable membrane performance.

Acknowledgements

This research work has been supported by the Spanish Research Foundation (CICYT Projects CTM2008-06809-C02-01 and CTM2008-06809-C02-02, and MICINN FPI grant BES-2009-023712) and Generalitat Valenciana (Projects GVA-ACOMP2010/130 and GVA-ACOMP2011/182), which are gratefully acknowledged.

Appendix

Distribution of the mean particle size in the anaerobic reactor mixed liquor (see Figure A.1).

References

[1] APHA (2005). Standard methods for the Examination of Water and Wastewater, 21st edition. American Public Health Association/American Water Works Association/Water Environmental Federation, Washington DC, USA.

[2] Bachin P., Aimar P., Sanchez V. (1995) Model for colloidal fouling of membranes. AIChE J. 41, 368 – 377.

[3] Bottino A., Capannelli G., Comite A. and Margano R. (2009) Critical flux in submerged membrane bioreactors for municipal wastewater treatment. Desalination 245, 748 – 753.

[4] Chang I. S., Clech P. L., Jefferson B. and Judd S. (2002) Membrane fouling in membrane bioreactors for wastewater treatment. J. Environ. Eng. 128, 1018 – 1029.

[5] Cho B.D. and Fane A.G. (2002) Fouling transients in nominally sub-critical flux operation of a membrane bioreactor. J. Membr. Sci. 209, 391 – 403

[6] Delgado S., Villaroel R. and González E. (2008) Effect of shear intensity on fouling in submerged membrane bioreactor for wastewater treatment. J. Membr. Sci. 311, 173 – 181.

[7] Dvořák L., Gómez M., Dvořáková M., Růžičková I. and Wanner J. (2011) The impact of different operating conditions on membrane fouling and EPS production. Bioresour. Technol. 102, 6870 – 6875.

[8] Field R.W., Wu D., Howell J.A., Gupta B.B. (1995) Critical flux concept for microfiltration fouling. J. Membr. Sci. 100, 259 – 272.

[9] Giménez J.B., Robles A., Carretero L., Durán F., Ruano M.V., Gatti M.N., Ribes J., Ferrer J. and Seco A. (2011) Experimental study of the anaerobic urban wastewater treatment in a submerged hollow-fibre membrane bioreactor at pilot scale. Bioresour. Technol. 102, 8799 – 8806.

[10] Guglielmi G. (2002) Membrane bioreactors for municipal wastewater treatment. Ph.D. thesis, Universita' di Trento, Italy.

[11] Guglielmi G., Chiarani D., Judd S.J. and Andreottola G. (2006) Flux criticality and sustainability in a hollow fibre submerged membrane bioreactor for municipal wastewater treatment. J. Membr. Sci. 289, 241 – 248.

[12] Guglielmi G., Saroj D. P., Chiarani D. and Andreottola G. (2007) Sub-critical fouling in a membrane bioreactor for municipal wastewater treatment: Experimental investigation and mathematical modelling. Water Res. 41, 3903 – 3914.

[13] Guo W.S., Vigneswaran S., Ngo H.H. and Xing W. (2008) Comparison of membrane bioreactor systems in wastewater treatment. Desalination 231, 61 – 70.

[14] Howell J.A., Chua H.C. and Arnot T.C. (2004) In situ manipulation of critical flux in a submerged membrane bioreactor using variable rates, and effects of membrane history. J. Membr. Sci. 242, 13 – 19.

[15] Jeison D. and van Lier J.B. (2006) Cake layer formation in anaerobic submerged membrane bioreactors (AnSMBR) for wastewater treatment. J. Membr. Sci. 284, 227 – 236.

[16] Jeison D. and van Lier J.B. (2007) Cake formation and consolidation: Main factors governing the applicable flux in anaerobic submerged membrane bioreactors (AnSMBR) treating acidified wastewaters. Sep. Purif. Technol. 56, 71 – 78.

[17] Judd S. (2010) The MBR Book: Principles and Applications of Membrane Bioreactors in Water and Wastewater Treatment, Second Edition, ELVESIER.

[18] Le-Clech P., Jefferson B., Chang I. S. and Judd S. (2003) Critical flux determination by the flux-step method in a submerged membrane bioreactor. J. Membr. Sci. 227, 81 – 93.

[19] Liao B.Q., Kraemer J.T. and Bagley D.M. (2006) Anaerobic membrane bioreactors: Applications and research directions. Crit. Rev. Env. Sci. Tec. 36, 489 – 530.

[20] Lin H.J., Xie K., Mahendran B., Bagley D.M., Leung K.T., Liss S.N., Liao B.Q. (2010) Factors affecting sludge cake formation in a submerged anaerobic membrane bioreactor. J. Membr. Sci. 36, 126 – 134.

[21] Rosenberger S., Laabs C., Lesjean B., Gnirss R., Amy G., Jekel M. and Schrotter J.C. (2006) Impact of colloidal and soluble organic material on membrane performance in membrane bioreactors for municipal wastewater treatment. Water Res. 40, 710 – 720.

[22] Stephenson, T., Judd, S., Jefferson, B., Brindle, K. (2000) Membrane Bioreactors for Wastewater Treatment. IWA publishing, London, UK.

[23] Vallero M. V. G., Lettinga G. and Lens P. N. L. (2005) High rate sulfate reduction in a submerged

anaerobic membrane bioreactor (SAMBaR) at high salinity. J. Membr. Sci. 253, 217 – 232.

[24] van der Marel P., Zwijnenburg A., Kemperman A., Wessling M., Temmink H. and van der Meer W. (2009) An improved flux-step method to determinate the critical flux and the critical flux for irreversibility in a membrane bioreactor. J. Membr. Sci. 332, 24 – 29.

[25] WRC (1992) Simple titration procedures to determine H2CO3* alkalinity and short-chain fatty acids in aqueous solutions containing known concentrations of ammonium, phosphate and sulphide weak acid/bases, Report No. TT 57/92, Water Research Commission, University of Cape Town, Pretoria, Republic of South Africa.

[26] Wu Z., Wang Z., Huang S., Mai S., Yang C., Wang X. and Zhou Z. (2008) Effects of various factors on critical flux in submerged membrane bioreactors for municipal wastewater treatment. Sep. Purif. Technol. 62, 56 – 63.

Figure and table captions

Figure 1. (a) General view of demonstration plant and **(b)** flow diagram. (Nomenclature: **RF**: rotofilter; **ET**: equalization tank; **AnR**: anaerobic reactor; **MT**: membrane tank; **DV**: degasification vessel; **CIP**: clean-in-place; **P**: pump; and **B**: blower).

Figure 2. Schematic representation of: **(a)** the modified flux-step method; **(b)** derived parameters; and **(c)** the increase in TMP at the same J between the upward flux-stepping and the downward flux-stepping.

Figure 3. Results of short-term trials with an SGD_m of 0.17, 0.33, and 0.5 $Nm^3\ h^{-1}\ m^{-2}$: **(a)** effect of J_{20} on TMP_{AVE}; and **(b)** effect of J_{20} on K_{AVE20}.

Figure 4. Results of short-term trials: **(a)** effect of J_{20} on membrane fouling rate with an SGD_m of 0.17, 0.23, 0.33, 0.4 and 0.5 $Nm^3\ h^{-1}\ m^{-2}$; **(b)** effect of SGD_m on J_{CW20}; and **(c)** effect of J_{CW20} on ΔTMP_{AVE}.

Figure 5. Long-term operating in sub-critical filtration conditions: **(a)** J_{20} of 10 LMH and SGD_m of 0.23 $Nm^3\ h^{-1}\ m^{-2}$; and **(b)** J_{20} of 13.3 LMH and SGD_m of 0.33 $Nm^3\ h^{-1}\ m^{-2}$.

Figure 6. Long-term operation: evolution during the operating period of TMP and MLTS. (Experimental period: **(i)** J_{20} of 13.3 LMH and temperature of 33 ºC; **(ii)** J_{20} of 10 LMH and temperature of 33 ºC; **(iii)** J_{20} of 12 LMH and temperature of 25 ºC; **(iv)** J_{20} of 13.3 LMH and temperature of 20 ºC; and **(v)** J_{20} of 11 LMH and ambient temperature (spring and summer season, from 20 to 30 ºC); and **(vi)** J_{20} of 9 LMH and ambient temperature (autumn and winter seasons, from 30 to 15 ºC)).

Table 1. Critical flux: some experimental values found in literature. (Nomenclature: **FS**: Flat-Sheet; **HF**: Hollow-Fibre; **MLTS**: mixed liquor total solids level; $\mathbf{J_{C,20}}$: 20 ºC-normalised critical flux; $\mathbf{U_G}$: upward gas/airflow velocity; **(A/G)R**: air/gas rate; and $\mathbf{S(A/G)D_m}$: specific air/gas demand per m^2 of membrane area).

(a)

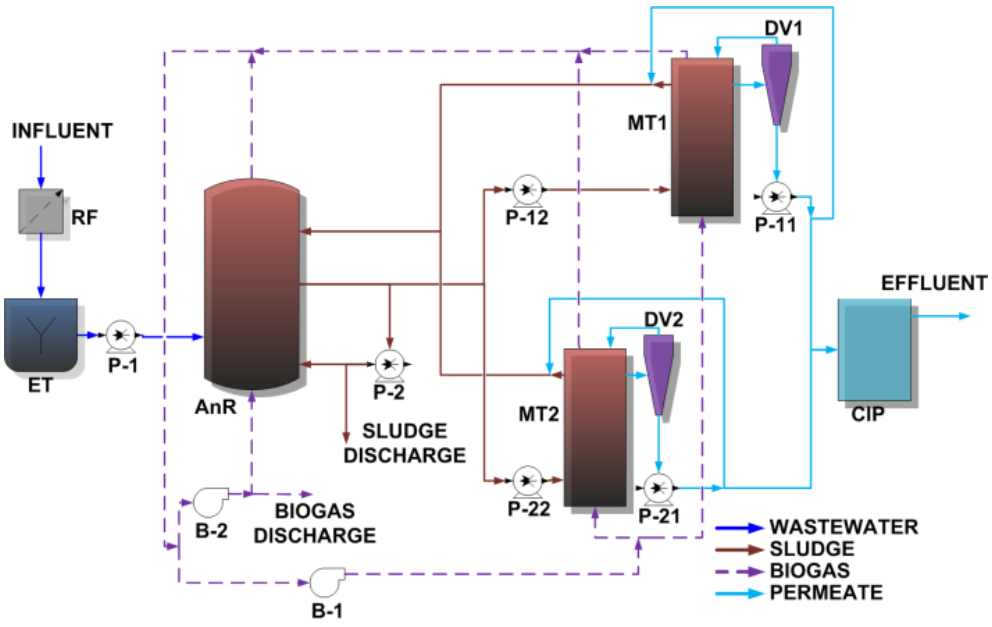

(b)

Figure 1. (a) General view of demonstration plant and **(b)** flow diagram. (Nomenclature: **RF**: rotofilter; **ET**: equalization tank; **AnR**: anaerobic reactor; **MT**: membrane tank; **DV**: degasification vessel; **CIP**: clean-in-place; **P**: pump; and **B**: blower).

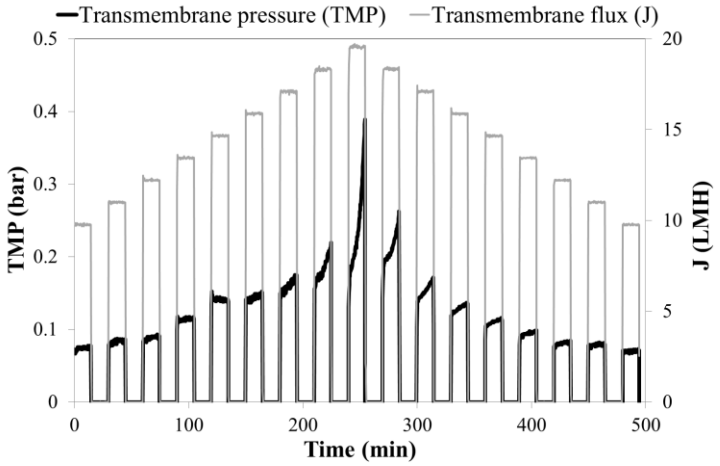
Transmembrane pressure (TMP)
Transmembrane flux (J)
TMP (bar)
J (LMH)
Time (min)
0
0.1
0.2
0.3
0.4
0.5
5
10
15
20
100
200
300
400
500

(a)

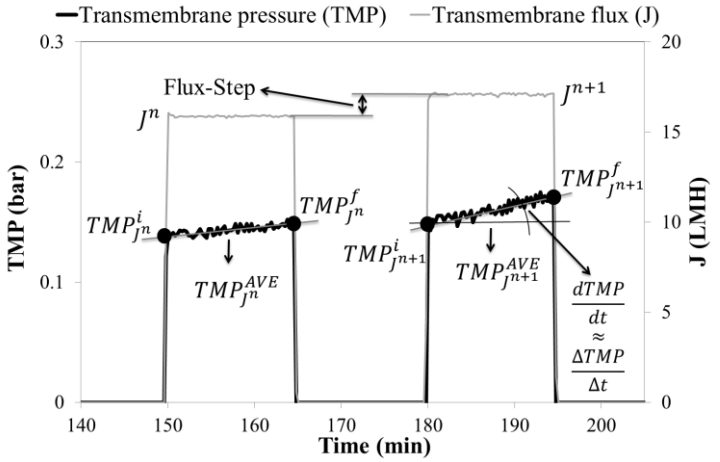
Transmembrane pressure (TMP)
Transmembrane flux (J)
Flux-Step
J^n
J^{n+1}
$TMP^i_{J^n}$
$TMP^f_{J^n}$
$TMP^{AVE}_{J^n}$
$TMP^i_{J^{n+1}}$
$TMP^f_{J^{n+1}}$
$TMP^{AVE}_{J^{n+1}}$
$\frac{dTMP}{dt} \approx \frac{\Delta TMP}{\Delta t}$
TMP (bar)
J (LMH)
Time (min)
0
0.1
0.2
0.3
5
10
15
20
140
150
160
170
180
190
200

(b)

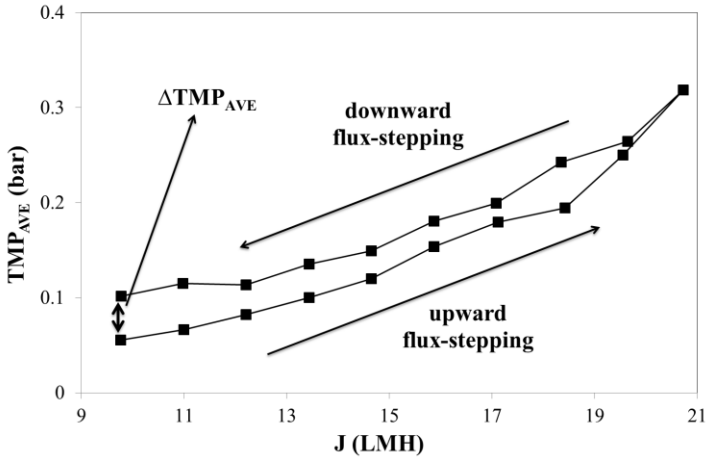

(c)

Figure 2. Schematic representation of: **(a)** the modified flux-step method; **(b)** derived parameters; and **(c)** the increase in TMP at the same J between the upward flux-stepping and the downward flux-stepping.

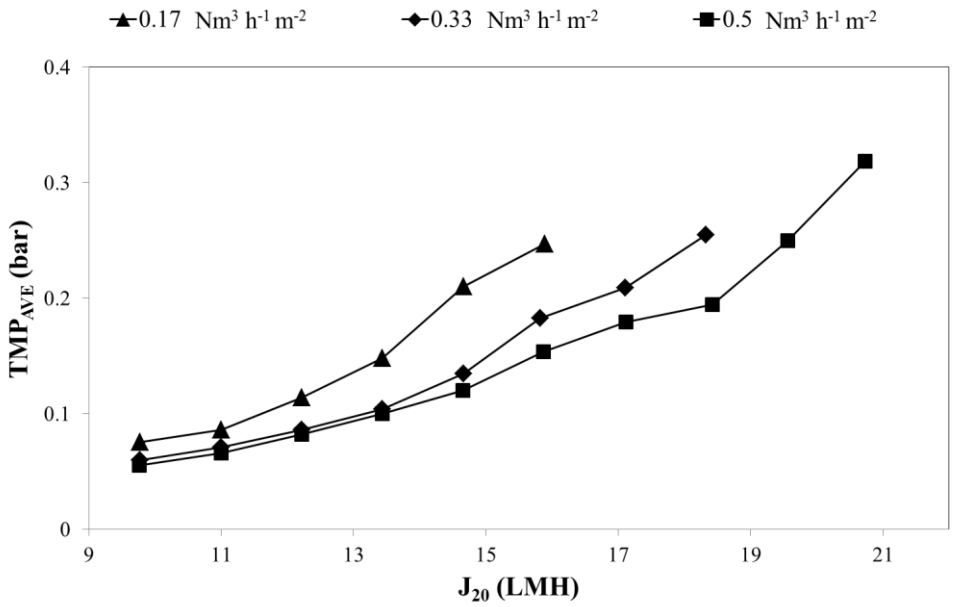

(a)

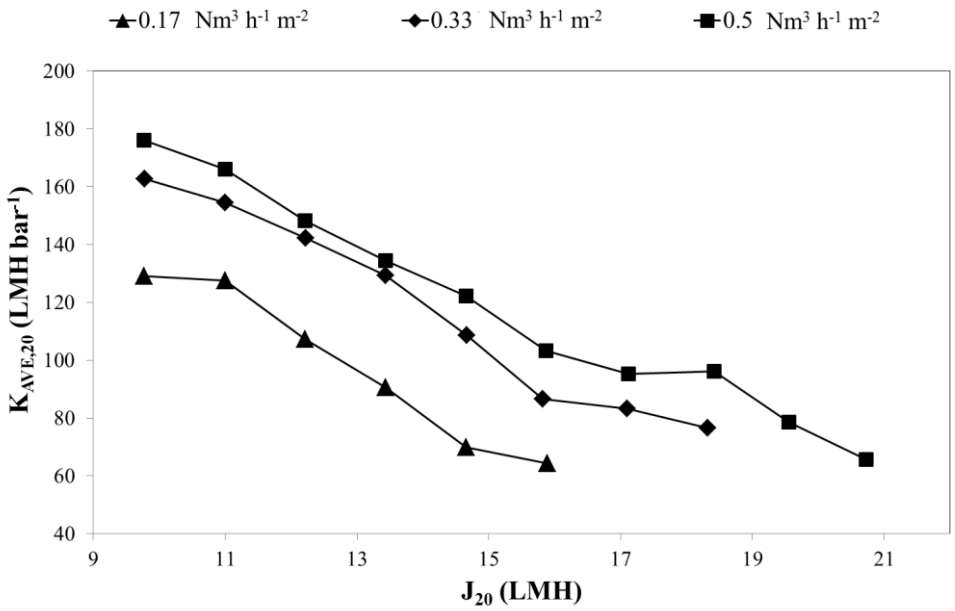

(b)

Figure 3. Results of short-term trials with an SGD_m of 0.17, 0.33, and 0.5 $Nm^3\ h^{-1}\ m^{-2}$: **(a)** effect of J_{20} on TMP_{AVE}; and **(b)** effect of J_{20} on K_{AVE20}.

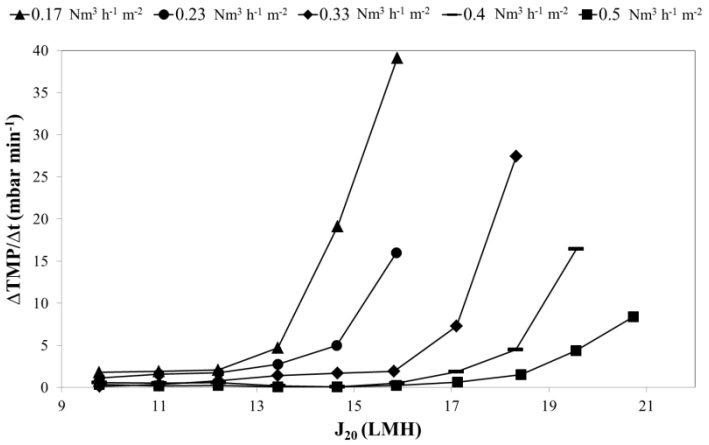

(a)

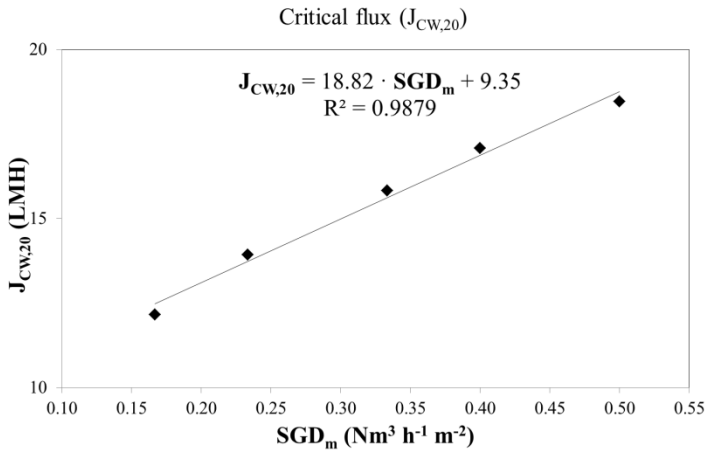

(b)

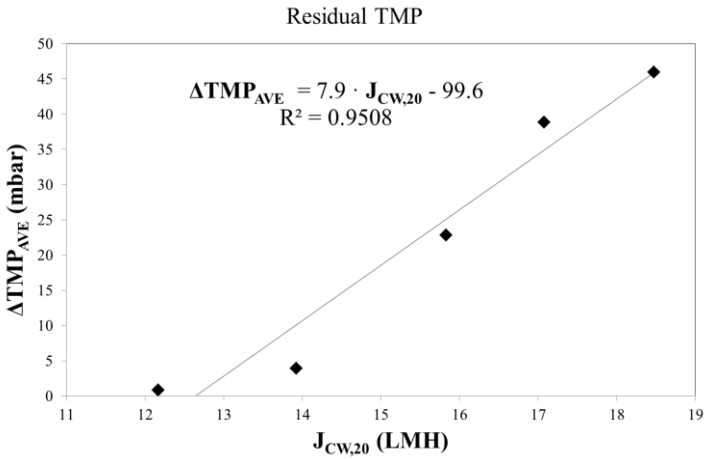

(c)

Figure 4. Results of short-term trials: **(a)** effect of J_{20} on membrane fouling rate with an SGD_m of 0.17, 0.23, 0.33, 0.4 and 0.5 $Nm^3\ h^{-1}\ m^{-2}$; **(b)** effect of SGD_m on J_{CW20}; and **(c)** effect of J_{CW20} on ΔTMP_{AVE}.

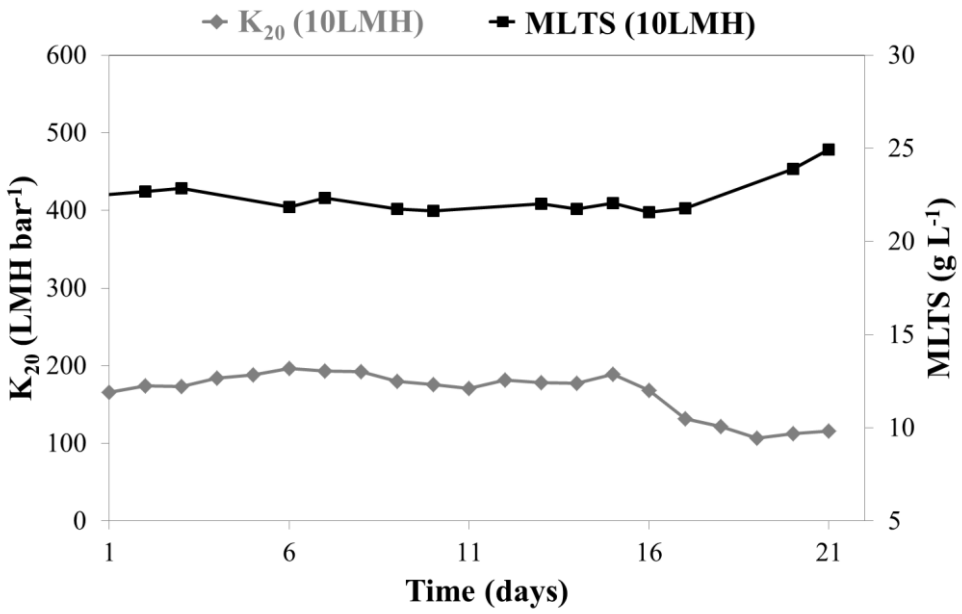

(a)

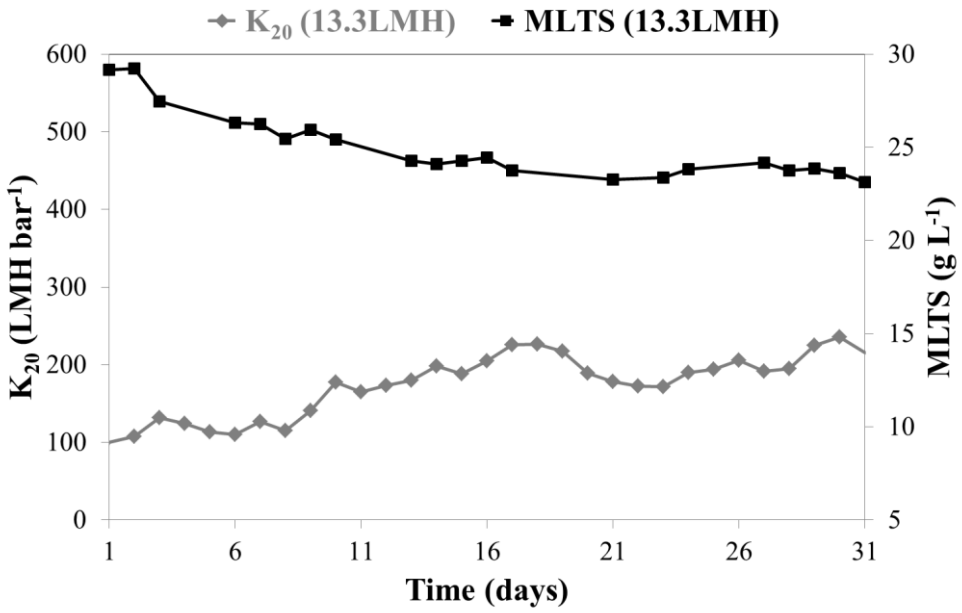

(b)

Figure 5. Long-term operating in sub-critical filtration conditions: **(a)** J_{20} of 10 LMH and SGD_m of 0.23 $Nm^3\ h^{-1}\ m^{-2}$; and **(b)** J_{20} of 13.3 LMH and SGD_m of 0.33 $Nm^3\ h^{-1}\ m^{-2}$.

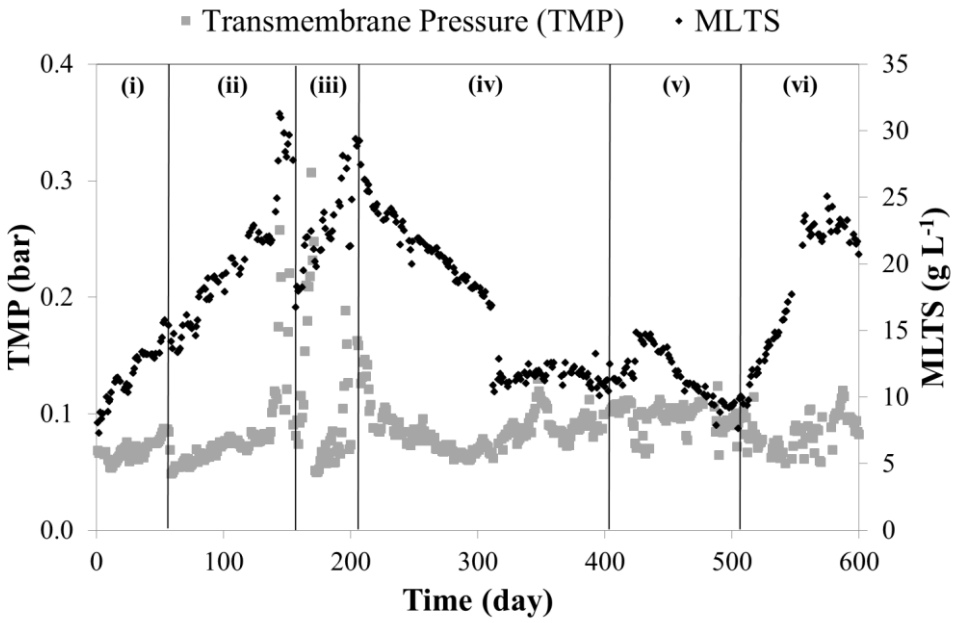

Figure 6. Long-term operation: evolution during the operating period of TMP and MLTS. (Experimental period: **(i)** J_{20} of 13.3 LMH and temperature of 33 ºC; **(ii)** J_{20} of 10 LMH and temperature of 33 ºC; **(iii)** J_{20} of 12 LMH and temperature of 25 ºC; **(iv)** J_{20} of 13.3 LMH and temperature of 20 ºC; and **(v)** J_{20} of 11 LMH and ambient temperature (spring and summer season, from 20 to 30 ºC); and **(vi)** J_{20} of 9 LMH and ambient temperature (autumn and winter seasons, from 30 to 15 ºC)).

Table 1. Critical flux: some experimental values found in literature. (Nomenclature: **FS**: Flat-Sheet; **HF**: Hollow-Fibre; **MLTS**: mixed liquor total solids level; **$J_{C,20}$**: 20 ºC-normalised critical flux; **U_G**: upward gas/airflow velocity; **(A/G)R**: air/gas rate; and **$S(A/G)D_m$**: specific air/gas demand per m^2 of membrane area).

Membrane (type)	Pore Size (μm)	Influent (type)	MBR (type)	MLTS ($g\ L^{-1}$)	$J_{C,20}$ (LMH)	U_G ($mm\ s^{-1}$)	(A/G)R ($Nm^3\ h^{-1}$)	$S(A/G)D_m$ ($Nm^3\ m^{-2}\ h^{-1}$)	Reference
FS	0.22	Synthetic	UASB	0.3 - 0.55	30 - 50	--	--	--	Cho *et al.*, 2002
FS	0.4	Synthetic	Aerobic	20	10 - 22	25 - 200	--	--	Howell *et al.*, 2004
FS	0.4	Municipal	Aerobic	8	17.5	--	1.5	8.6	Wu *et al.*, 2008
FS	0.8	Municipal	Aerobic	8	29.5	--	1.5	8.6	Wu *et al.*, 2008
FS	0.2	Municipal	Aerobic	8	41.5	--	1.5	8.6	Wu *et al.*, 2008
FS	0.45	Synthetic	Aerobic	10	25	300 - 600	--	--	Guo *et al.*, 2008
FS	0.37	Municipal	Aerobic	14	5	--	0.18	--	Bottino *et al.*, 2009
FS	0.1	Municipal	Aerobic	10	50	--	0.4	--	van der Marel *et al.*, 2009
Tubular	0.2	Synthetic	Aerobic	3	10	--	0.36	1.9	Le-Clech *et al.*, 2003
Tubular	0.2	Municipal	Aerobic	3	10	--	0.36	1.9	Le-Clech *et al.*, 2003
Tubular	0.2	Synthetic	Anaerobic	25	16 - 22	97 - 195	--	--	Guglielmi *et al.*, 2006
Tubular	0.2	Synthetic	Anaerobic	35	3 - 6	55 - 195	--	--	Jeison *et al.*, 2007
HF	0.1	Domestic	Aerobic	12 - 19	19	--	--	--	Guglielmi *et al.*, 2002
HF	0.4	Domestic	Aerobic	10 - 18	20	--	--	--	Guglielmi *et al.*, 2002
HF	0.04	Municipal	Aerobic	10	25 - 31	--	20.9 - 69.6	0.3 - 1.0	Stephenson *et al.*, 2000
HF	0.04	Municipal	Aerobic	10	28	--	37.8	0.35	Guglielmi *et al.*, 2007
HF	0.05	Municipal	Anaerobic	23	12 - 19	50 - 160	5 - 15	0.17 - 0.5	Our study